An Ancient Protein Phosphatase, SHLP1, Is Critical to Microneme Development in *Plasmodium* Ookinetes and Parasite Transmission

Eva-Maria Patzewitz,[1,6] David S. Guttery,[1,6] Benoit Poulin,[1,6] Chandra Ramakrishnan,[2] David J.P. Ferguson,[3] Richard J. Wall,[1] Declan Brady,[1] Anthony A. Holder,[4] Balázs Szöőr,[5] and Rita Tewari[1,*]

[1]Centre for Genetics and Genomics, School of Biology, Queens Medical Centre, University of Nottingham, Nottingham NG2 7UH, UK
[2]Division of Cell and Molecular Biology, Imperial College London, London SW7 2AZ, UK
[3]Nuffield Department of Clinical Laboratory Science, University of Oxford, John Radcliffe Hospital, Oxford OX3 9DU, UK
[4]Division of Parasitology, MRC National Institute for Medical Research, Mill Hill, London NW7 1AA, UK
[5]Institute of Immunology and Infection Research, School of Biological Sciences, University of Edinburgh, Edinburgh EH9 3JT, UK
[6]These authors contributed equally to this work
*Correspondence: rita.tewari@nottingham.ac.uk
http://dx.doi.org/10.1016/j.celrep.2013.01.032

SUMMARY

Signaling pathways controlled by reversible protein phosphorylation (catalyzed by kinases and phosphatases) in the malaria parasite *Plasmodium* are of great interest, for both increased understanding of parasite biology and identification of novel drug targets. Here, we report a functional analysis in *Plasmodium* of an ancient bacterial *Shewanella*-like protein phosphatase (SHLP1) found only in bacteria, fungi, protists, and plants. SHLP1 is abundant in asexual blood stages and expressed at all stages of the parasite life cycle. *shlp1* deletion results in a reduction in ookinete (zygote) development, microneme formation, and complete ablation of oocyst formation, thereby blocking parasite transmission. This defect is carried by the female gamete and can be rescued by direct injection of mutant ookinetes into the mosquito hemocoel, where oocysts develop. This study emphasizes the varied functions of SHLP1 in *Plasmodium* ookinete biology and suggests that it could be a novel drug target for blocking parasite transmission.

INTRODUCTION

Unicellular parasites of the genus *Plasmodium* are the causative agent of malaria, with annual fatalities close to 1.25 million (Murray et al., 2012). Development of mammalian *Plasmodium* species proceeds via asexual exoerythrocytic proliferation and intraerythrocytic multiplication occurring in mammalian liver hepatocytes and erythrocytes, respectively, whereas sexual development and sporogony occur in the mosquito. *Plasmodium* belongs to the phylum Apicomplexa, which is characterized by the presence of distinct apical organelles consisting of micronemes, dense granules, and rhoptries that are used by the parasite for host invasion and gliding motility (Bannister and Sherman, 2009). Of the three invasive stages (sporozoites, merozoites, and ookinetes), the ookinete uniquely lacks rhoptries and dense granules.

In most organisms, processes involved in cell cycle, differentiation, and development are regulated by reversible phosphorylation of proteins. While kinases are well recognized as important drug targets, the study of protein phosphatases (PPs) has only recently begun to identify them as potential therapeutic targets (McConnell and Wadzinski, 2009; Moorhead et al., 2007).

Bioinformatic analyses have identified ∼80 kinases and ∼30 PP catalytic subunits encoded in the *P. falciparum* genome (Ward et al., 2004; Wilkes and Doerig, 2008), compared to 518 kinases and 147 PP catalytic subunits identified in the human genome (Moorhead et al., 2007). Recent systematic functional studies have uncovered the important roles of kinases during signal transduction and various developmental processes in *Plasmodium* (Solyakov et al., 2011; Tewari et al., 2010).

Although complementary functional studies of the *Plasmodium* phosphatome are lacking, its bioinformatic analysis has revealed the presence of nonconventional PPs containing kelch-like motifs as found in plant PPs and two bacterial *Shewanella*-like PPs (Shelphs or SHLP), both lacking orthologs in humans (Wilkes and Doerig, 2008). SHLPs are related to the phosphoprotein phosphatase (PPP) family of serine/threonine PPs (STPs), span the eukaryote-prokaryote boundary, and are also present in plants, heterokonts, fungi, and some *Protozoa* (Andreeva and Kutuzov, 2004; Uhrig and Moorhead, 2011).

In *Plasmodium*, the expression of its two SHLP isoforms in late schizont and merozoite stages has been reported (Hu et al., 2010). Although the γ-proteobacterium *Shewanella* spp. SHLP has been utilized to analyze enzymatic catalysis at low temperatures (Tsuruta et al., 2008), no function of any SHLP is known to date (Kutuzov and Andreeva, 2012).

In this study, we have used the rodent malaria *P. berghei* to elucidate the function of *Plasmodium* SHLP1 (PBANKA_133240) during the parasite life cycle using reverse genetics, biochemical and cell biological approaches.

RESULTS AND DISCUSSION

Bioinformatics of *Shewanella*-like Protein Phosphatases in *Plasmodium*

We confirmed the presence of two genes in the *P. berghei* genome encoding *Shewanella*-like PPs: PBANKA_133240, which has a signal peptide and apicoplast targeting sequence and PBANKA_060470, which were named *Shewanella*-like protein phosphatases SHLP1 and SHLP2, respectively.

In eukaryotes other than in *Apicomplexa*, SHLPs have been found in, *Archaeplastida*, some fungi, and some *Chromalveolates* and are structurally related to a class of bacterial PPPs first identified in the psychrophilic bacteria *Shewanella* and *Colwellia* (Tsuruta et al., 2008). Consequently, a phylogenetic tree was constructed from multiple alignments of 47 SHLP-related amino acid sequences (Figure 1A; Table S1) that confirmed the presence of SHLPs in the examined species in addition to flowering plants (Kutuzov and Andreeva, 2012; Uhrig and Moorhead, 2011). Both PbSHLP1 and PbSHLP2 show higher identity to AtSLP2 than AtSLP1 (Table S1) and form a distinct phylogenetic group in *Chromalveolata*.

Plasmodium spp. contained two SHLPs, while *Toxoplasma* and *Cryptosporidium* have only one SHLP mostly resembling SHLP2. Sequence analysis of *Plasmodium* SHLPs revealed that only the highly conserved STP catalytic residues (GD[I/V/T/L]HG, GD[L/Y/F]V[D/A]RG, GNHE, HGG) and metal ion binding sites (underlined) are largely conserved. The rest of the conserved STP residues, okadaic acid, and microcystin LR inhibitor binding sites, as well as PP1 regulatory subunit binding sites (K[I]F, E[FF]) and PP1 substrate binding sites are only partially or not conserved (Figure S1). Amino acids involved in PP2A trimeric holoenzyme formation were also absent (Figure S1).

SHLP1-GFP Is Present in All the Parasite Developmental Stages Examined, Is Preferentially Localized to the Endoplasmic Reticulum, and Is Present in Membrane Fractions

To study its expression during the *P. berghei* life cycle, we generated a C-terminal GFP fusion protein using endogenous *shlp1* (PBANKA_133240) and single crossover recombination (Figures S2A–S2C). SHLP1-GFP showed diffuse fluorescence staining in all parasite stages examined by microscopy with prominent staining in the asexual stages, the male gamete, and oocyst (Figure 1B). However, despite the presence of a predicted apicoplast targeting signal, the protein was found distributed nonuniformly throughout the parasite body in all stages analyzed (Figure 1B) and colocalized with ER tracker Red, suggesting that SHLP1-GFP is located in the endoplasmic reticulum (ER) (Figure 1C). This was further confirmed by high-resolution imaging (Figure S1B). Furthermore, subcellular fractionation of asexual blood stages using hypotonic lysis and carbonate solubility recovered most of the SHLP1-GFP protein in the carbonate soluble (peripheral membrane) and carbonate insoluble (integral membrane proteins) fractions, suggesting a membrane localization of the protein in the ER. GFP alone in the control was in the soluble (cytosolic) fraction and GAP45 control was found in the integral membrane fraction (Figure 1D).

A cytosolic localization has recently been described for AtSLP2 (At1g18480), whereas AtSLP1 was located in the chloroplast (Uhrig and Moorhead, 2011); *P. falciparum* SHLP2 (PF3D7_1206000) was recently identified at the apical end of the merozoite (Hu et al., 2010).

SHLP1 Has Phosphatase Enzyme Activity and Is Not Itself Phosphorylated in Schizonts or Activated Gametocytes

We investigated whether SHLP1 is an active phosphatase in *P. berghei* using the SHLP1-GFP protein expressed in vivo and 3-O-methylfluorescein phosphate (MFP) as a substrate. SHLP1-GFP displayed phosphatase activity proportional to the amount of lysate in the assay; wild-type (WT) parasite extracts not expressing GFP and WT and SHLP1-GFP controls without MFP substrate produced almost no signal. The basal fluorescence level observed in GFP control lysates was likely due to GFP fluorescence, as the signal was still present in the absence of MFP substrate (Figure 2A, upper panel). Unlike classical eukaryotic PPP, which are specific for Ser and Thr residues, bacterial PPPs may have broader substrate specificity, and the cold-active phosphatase originally described in *Shewanella* is a Tyr PP (Tsuruta et al., 2008). MFP is hydrolyzed by both Ser/Thr- and Tyr-specific PPs, and, since SHLP1 is related to the STP family of PPs, we tested for activity in the presence of the PPP inhibitors okadaic acid and microcystin-LR. SHLP1-GFP phosphatase activity was not affected by either inhibitor (Figure 2A, lower panel left), consistent with previous studies with AtSLPs (Uhrig and Moorhead, 2011) and predictions from our bioinformatic analysis (Figure S1) that *Plasmodium* SHLP1 is divergent in the residues involved in inhibitor binding to type 1 PPs. A PP2A enzyme was used as a positive control in the same assay conditions, and its activity was almost abolished by both inhibitors (Figure 2A, lower panel right).

As a number of PPs are known to be regulated by phosphorylation (Mochida and Hunt, 2012), we analyzed SHLP1-GFP phosphorylation in vivo. Although activated gametocytes and schizonts from WT-GFP- and SHLP1-GFP-expressing parasite lines incorporated ^{32}P-orthophosphate into the total complement of proteins (Figure 2B, upper panel), SHLP1-GFP was not phosphorylated at either stage (Figure 2B, middle panel, arrow), though detectable by western blot (Figure 2B lower panel), consistent with data from previous global phosphoproteomics studies of *P. falciparum* schizonts (Lasonder et al., 2012).

SHLP1 Is Critical to Ookinete Formation, Ookinete-to-Oocyst Transition, and Parasite Transmission

To elucidate the function of SHLP1 during the *Plasmodium* life cycle, we replaced the endogenous *shlp1* gene with a *T. gondii dhfr/ts* selectable marker using double homologous recombination (Figures S2D–S2H). Analysis of two deletion mutant clones from two independent transfections identified no phenotypic differences from WT parasites during asexual stages or gametocytogenesis, as assessed on blood smears (data not shown).

Microgametogenesis as assessed by exflagellation was comparable to that of WT parasites (Figure 3A). Analysis of zygote formation and ookinete development postfertilization in vitro
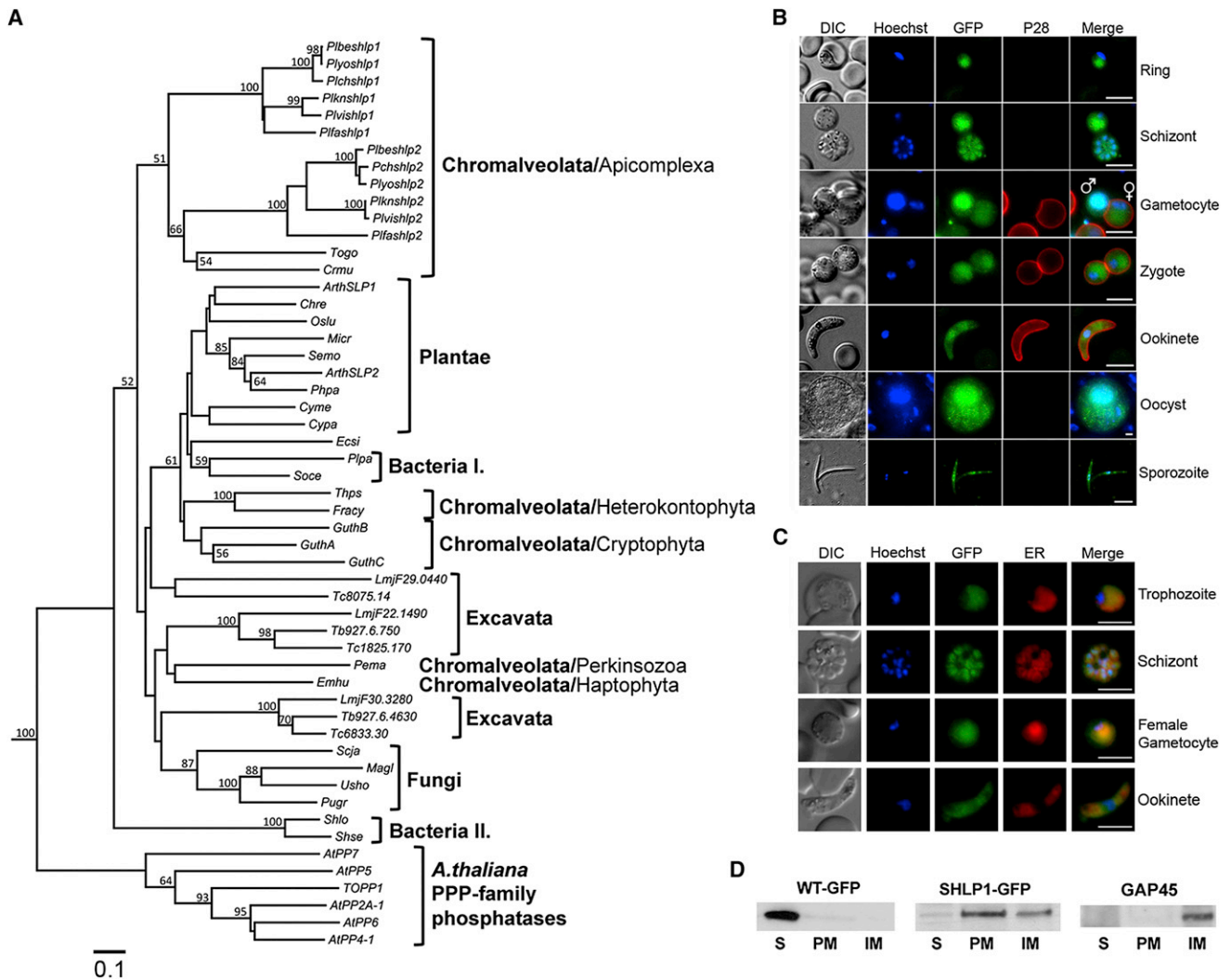
Figure 1. Phylogenetic Analysis and Expression of SHLP1 during Parasite Development

(A) Multiple alignment of the catalytic domains of SHLP proteins excluding positions with a gap in any sequence was used to construct a phylogenetic tree by the neighbor-joining method and using Kimura's empirical correction for multiple hits with 100 bootstrapped replicates implemented in ClustaW2. The PP catalytic domains were identified by the conserved PPP specific motifs "GD(L/I/V)HG" at the N-terminal and the "(I/L/V)D(S/T/G)" at the C-terminal region. *A. thaliana* PPP family PPs were used as an out group in the analysis. Species and gene abbreviations are outlined in Table S1. Trypanosome *T. brucei* (*Tb*), *T. cruzi* (*Tc*), and *L. major* (*Lmj*) PP domains are indicated by systematic gene IDs. Bootstrap values of 50% and above for the nodes are shown. The scale bar indicates 0.1 substitutions per site.

(B) SHLP1-GFP expression in transgenic parasites. A Cy3-conjugated antibody recognizing P28 on the surface of activated females, zygotes, and ookinetes was used in the sexual stages. Scale bar, 5 μm.

(C) Costaining with ER-tracker Red shows association of SHLP1-GFP with the ER. Scale bar, 10 μm.

(D) WT-GFP and SHLP1-GFP subcellular fractionation. Anti-GFP (left two panels) and anti-GAP45 (right panel) western blot of soluble (S), peripheral membrane (PM), and integral membrane (IM) fractions.

See also Figure S1.

revealed a significant reduction (55%–60%) in ookinete conversion in Δshlp1 parasites (Figure 3B). Time-course analysis revealed that ookinete formation and differentiation was reduced from the onset in Δshlp1 mutants (9 hr postfertilization) and thus was not a result of parasite death or dedifferentiation of ookinetes before they reached full maturity at 24 hr (Figure 3C), in contrast to a previously described phosphodiesterase (*pdeδ*)-deficient parasite (Moon et al., 2009). This suggests that

SHLP1 plays an important (though not essential) role at an early stage in ookinete development and differentiation.

For ookinetes that did fully differentiate, we analyzed their motility (Moon et al., 2009) and found that gliding motility in Δshlp1 ookinetes was indistinguishable from that of WT parasites (Figure 3D; Movies S1 and S2), indicating that their motor function was unimpaired. Parasite motility is governed by an actomyosin motor termed the glideosome, which resides within
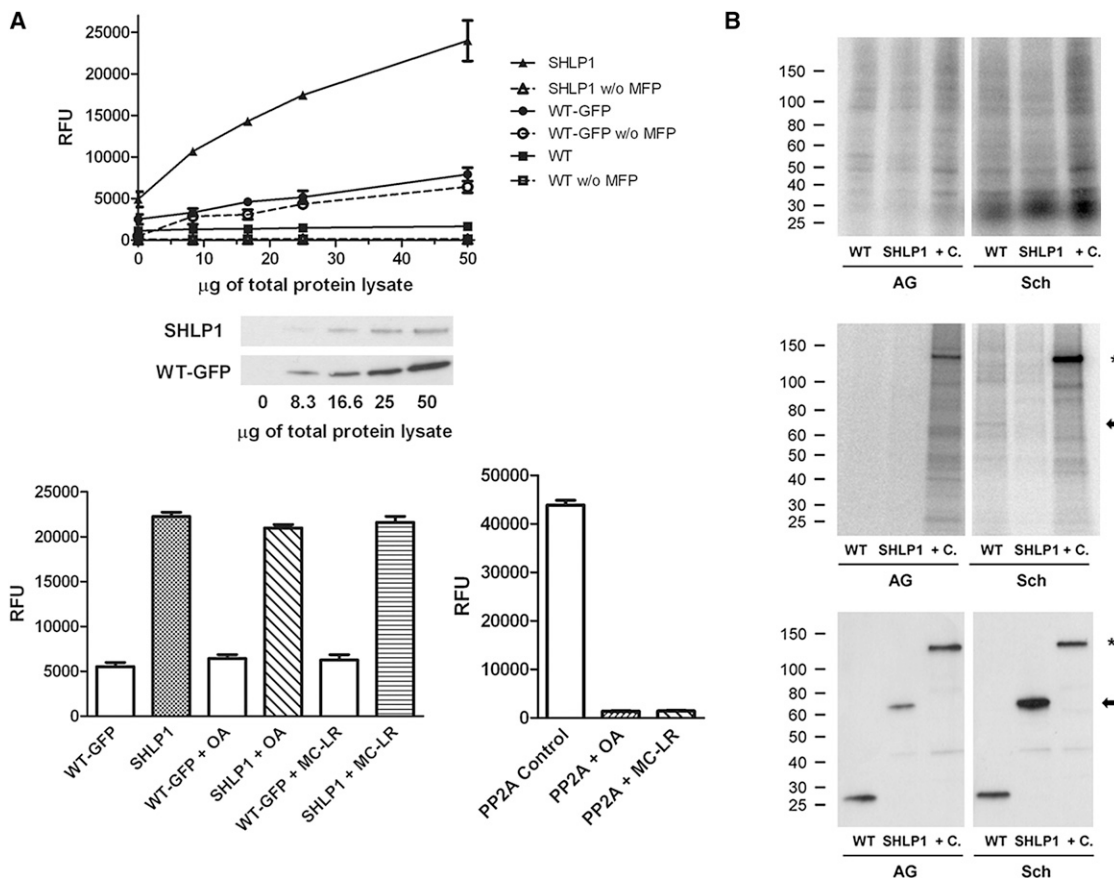
Figure 2. SHLP1-GFP Phosphatase Activity and In Vivo Phosphorylation Levels

(A) Upper panel: phosphatase activity in immunoprecipitates from lysates of SHLP1-GFP, WT-GFP, and WT parasite lines with or without MFP substrate and anti-GFP western blot showing amounts of SHLP1-GFP and WT-GFP retained from the corresponding lysates. Lower panel: phosphatase activity of the same immunoprecipitates (left, from 30 μg total protein) and of recombinant PP2A control (right, 0.1 U) in the presence or absence of okadaic acid (OA, 120 nM) and microcystin-LR (MC-LR, 10 nM). Error bar ±SEM, n = 3.

(B) Upper panel: autoradiograph of ^{32}P-labeled total protein lysates before immunoprecipitation in activated gametocytes (AG) and schizonts (Sch) from WT-GFP, SHLP1-GFP, and PPKL-GFP (+C) parasites. Middle panel: autoradiograph showing phosphorylation of GFP-TRAP immunoprecipitated lysates. Lower panel: corresponding western blot using anti-GFP antibody on the immunoprecipitates. Arrow shows the position of SHLP1-GFP on the gels, and the star marks the position of phosphorylated PPKL-GFP (Guttery et al., 2012b).

the pellicle of invasive zoites (Opitz and Soldati, 2002). Motility and midgut invasion by the ookinete involves the secretion of a number of membrane proteins, micronemal proteins such as circumsporozoite and TRAP-related protein (CTRP) (Dessens et al., 1999; Yuda et al., 1999), and secreted ookinete adhesive protein (SOAP) (Dessens et al., 2003), as well as the action of the calcium-dependent protein kinases, CDPK3 (Siden-Kiamos et al., 2006) and CDPK1 (Sebastian et al., 2012).

To extend these findings in vivo, *A. stephensi* mosquitoes were fed on mice infected with either WT or Δ*shlp1* parasites to analyze both oocyst development and sporogony. While the WT developed normally, no Δ*shlp1* oocysts were found on day 14 or 21 postinfection (p.i.) (Figure 3E). Hence, to determine whether the lack of oocyst formation in Δ*shlp1* mutant parasites was due to a defect in invasion of the midgut epithelium, we bypassed the midgut barrier by injecting ookinetes directly into the hemocoel of *A. stephensi* mosquitoes and analyzed salivary

glands for sporozoites 20 days postinjection (Ecker et al., 2008). Δ*shlp1* parasites were able to form viable sporozoites, which could migrate to and actively invade the salivary gland (Figure 3F). Parasite transmission experiments using these mosquitoes resulted in infection of mice with both WT and Δ*shlp1* lines, strongly suggesting that the mutant parasites undergo normal exo- and intraerythrocytic proliferation, but oocyst development in vivo is ablated. Subsequent in vivo invasion assays using *A. gambiae* L3-5 mosquitoes (Collins et al., 1986) with WT and Δ*shlp1* parasites showed a slight but nonsignificant reduction in melanized Δ*shlp1* ookinetes compared to WT (Figure S3A). These data indicate that Δ*shlp1* ookinetes are able to cross the midgut epithelium but cannot form oocysts.

SHLP1 Function Is Contributed by the Female Gamete

We next examined whether the defect was sex specific by performing genetic crosses between Δ*shlp1* parasites and lines
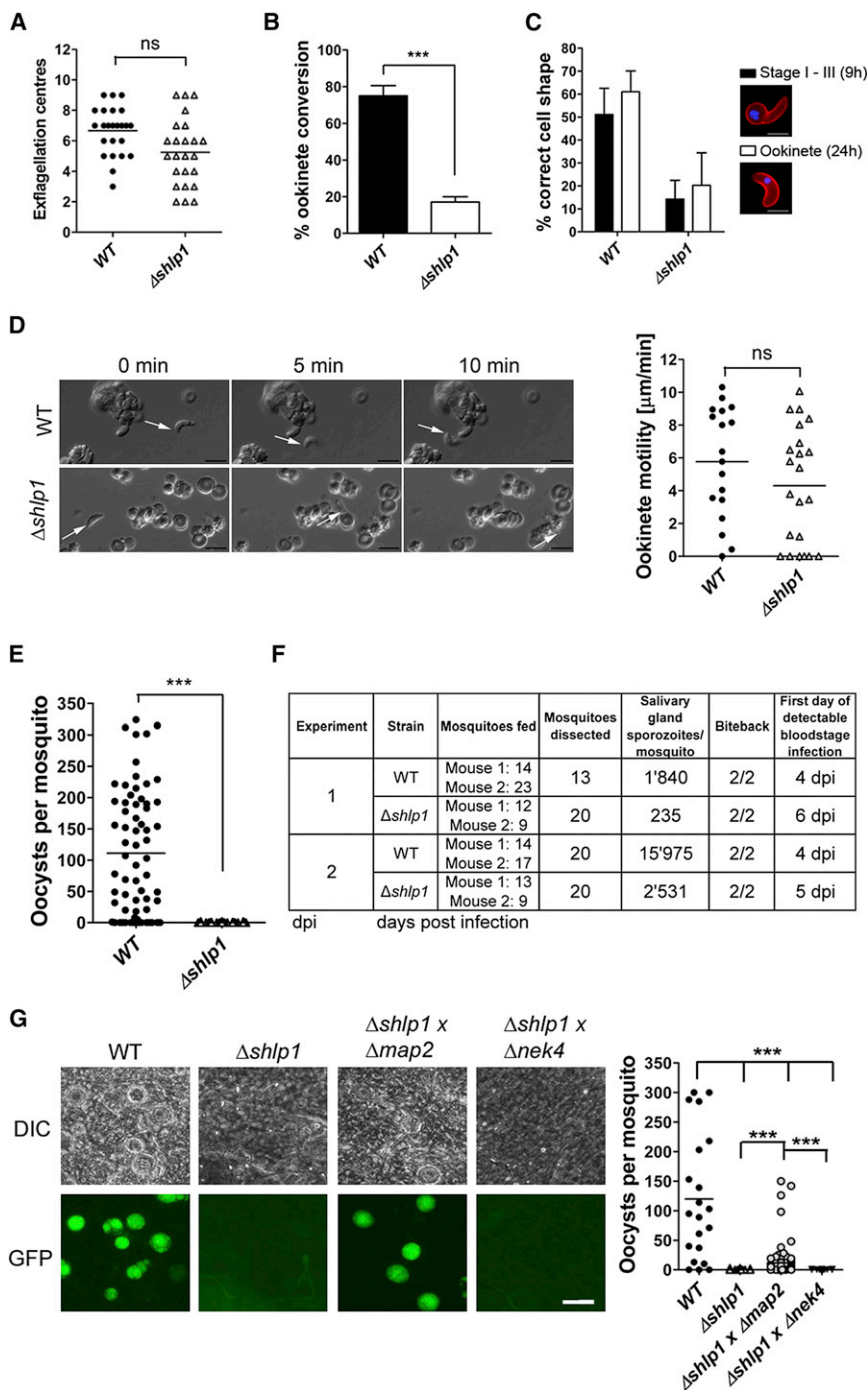
Figure 3. Phenotypic Analyses of Δ*shlp1* Mutants: Ookinete Formation and Oocyst Development Are Affected

(A) Microgametogenesis in WT and Δ*shlp1* mutant lines measured as number of exflagellation centers (ns = not significant, Mann-Whitney U test, p > 0.05).

(B) Ookinete conversion in Δ*shlp1* mutants compared to WT (Mann-Whitney U test, ***p < 0.001). Data shown as mean ±SD.

(C) Developing ookinete stages shown as the percentage of female-derived cells for WT and Δ*shlp1* with the correct shape at either 9 hr (stages I–III) or 24 hr (fully differentiated ookinete) post-fertilization. Data shown as mean ±SD.

(D) Representative frames from time-lapse movies of WT (upper panels) and Δ*shlp1* (lower panels) ookinetes in Matrigel. Arrow indicates the apical end of the ookinete. Bar = 10 μm. Velocity of individual WT or Δ*shlp1* ookinetes from 24 hr cultures was measured over 10 min, as shown in the dot plot. Bar = arithmetic mean; n = 18 for WT and 22 for Δ*shlp1* lines.

(E) Numbers of oocysts in *A. stephensi* midguts on day 14 postblood feeding show complete ablation of oocyst development in Δ*shlp1* parasites compared to WT (Mann-Whitney U test, ***p < 0.001).

(F) Hemocoel injection of Δ*shlp1* ookinetes shows that mutant sporozoites invade the salivary glands, can be successfully transmitted to mice, and are able to establish new infections.

(G) Genetic complementation of Δ*shlp1* parasites. Mosquitoes were fed on mice infected with WT or Δ*shlp1* mutant alone or coinfected with Δ*shlp1* and either a Δ*map2* mutant or a Δ*nek4* mutant. Scale bar, 100 μm (Kruskal-Wallis test, ***p < 0.001).
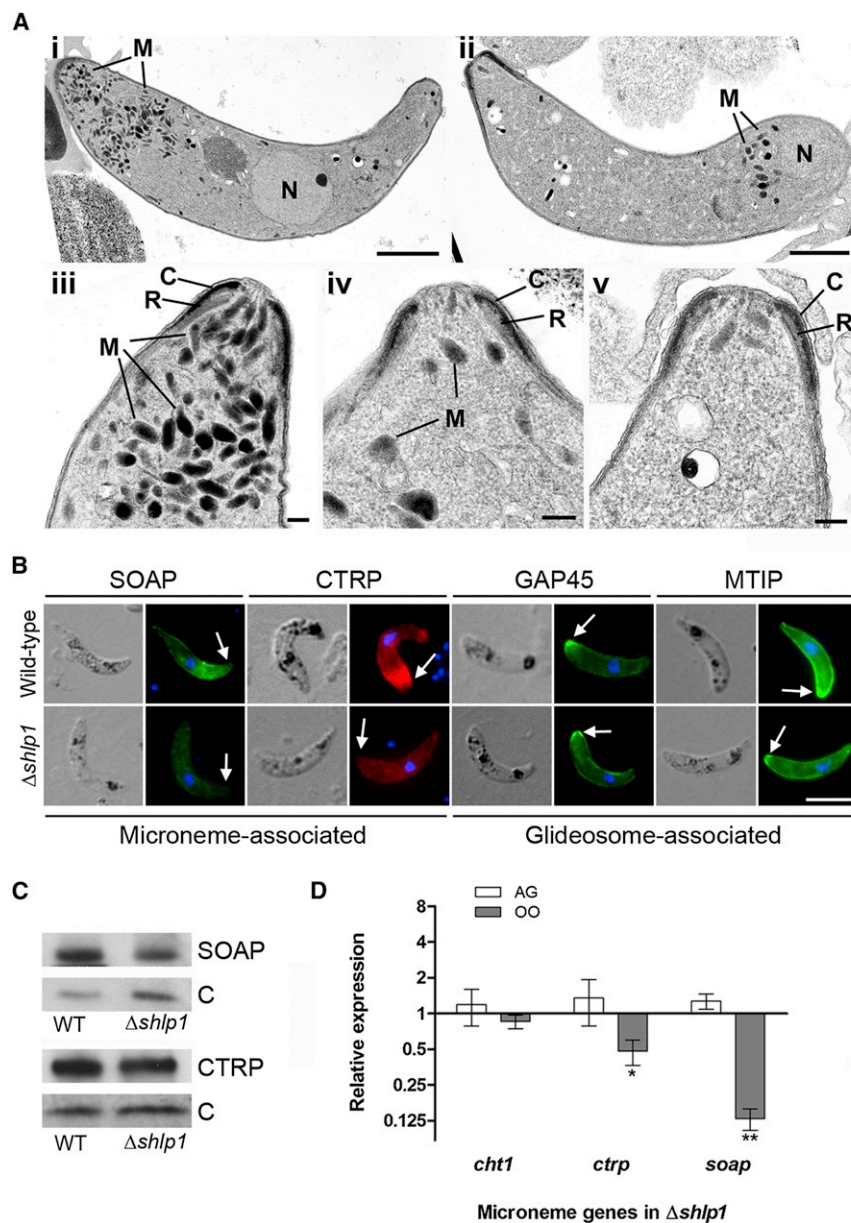
See also Figure S2.

SHLP1 Is Important for Microneme Formation in Ookinetes

To identify whether deletion of *shlp1* results in morphological defects in the viable ookinetes at the ultrastructure level, we analyzed Δ*shlp1* parasites using transmission electron microscopy (TEM). While no defects were found in the apical architecture of Δ*shlp1* ookinetes (i.e., the plasmalemma, inner membrane complex [IMC], central aperture, and subpellicular microtubules) (Figures 4Ai–4Aiii and S3B), there was a marked reduction in the number of apical micronemes (Figures 4Aii, 4Aiv, 4Av, and S3B). Of the various sections examined, 80%–90% of Δ*shlp1* ookinetes had either no apical micronemes (Figures 4Aiv, 4Av, and S3B) or had markedly reduced microneme numbers, which were not apically located (Figures 4Aiv and S3B).

For confirmation, we performed indirect immunofluorescence and western blotting for proteins associated with either the ookinete motor complex or the micronemes (Figure 4B). While the

deficient in either male (Δ*map2*) or female (Δ*nek4*) gametes (Tewari et al., 2010). We found that only the Δ*map2* mutant was able to rescue the Δ*shlp1* phenotype and form oocysts in the mosquito midgut (p < 0.001), confirming a strict requirement for a functional female copy of the *shlp1* gene. Ookinetes resulting from female gametocytes with this genotype can be complemented by mutant parasites with viable female forms (Figure 3G).

Figure 4. Microneme Reduction and Mislocalization in Δshlp1 Ookinetes

(A) (i) Transmission electron micrograph (TEM) of a longitudinal section through a WT ookinete showing the conical apical end. The cytoplasm contains a number of apically located micronemes (M) and a more posteriorly located nucleus (N). Scale bar, 1 μm. (ii) Longitudinal TEM section through a Δshlp1 ookinete showing substantial reduction of micronemes and mislocalization of remaining micronemes at the posterior end. Bar = 1 μm. (iii) Enlargement of the anterior of a WT ookinete showing the complex nature of the apical end consisting of a conical shaped electron dense collar (C) with a central aperture and an underlying less electron dense ring (R). Micronemes (M) are located within the cytoplasm. Scale bar, 100 nm. (iv and v). Detail of the anterior of Δshlp1 ookinetes showing reduction in micronemes (M). Scale bar, 100 nm.

(B) Indirect immunofluorescence of a number of motor complex and micronemal proteins in WT and Δshlp1 ookinetes. Compared to WT, staining for micronemal proteins SOAP and CTRP was reduced in the Δshlp1 mutant and spread throughout the cell body as opposed to the normal concentration at the apical end (arrow). No difference was observed between WT and mutant ookinetes for glideosomal GAP45 and MTIP.

(C) Western blot analyses of ookinete micronemal proteins CTRP and SOAP. Expression levels were compared between WT and Δshlp1 ookinetes and normalized to the GFP control using ImageJ software. CTRP expression was unaltered in the mutant whereas SOAP expression was reduced to 40%.

(D) Relative RNA expression of microneme specific genes *cht1*, *ctrp, and soap* in Δshlp1 mutant parasites compared to WT controls. Each point is the mean of three biological replicates ±SD (normalized using qBasePlus). AG, activated gametocytes; OO, ookinete. *$p < 0.05$; **$p < 0.01$. See also Figure S3.

glideosome-associated protein 45 (GAP45) and myosin A tail domain-interacting protein (MTIP) displayed no obviously abnormal pattern in the Δshlp1 line, micronemal CTRP showed a less distinct apical staining and overall a less intense staining distributed throughout the body of the ookinete relative to that of the WT. Similar differences were observed for micronemeassociated SOAP consistent with the marked reduction of micronemes in Δshlp1 ookinetes observed by TEM. However, western blot analysis of CTRP and SOAP revealed that overall levels of CTRP were comparable between mutant and WT, whereas SOAP was reduced in the Δshlp1 ookinete to 40% of WT levels (Figure 4C).

The RNA expression profile for female-specific and micronemal genes was comparable for all genes analyzed in WT parasites with the exception of *soap,* which appeared to be upregulated by 2-fold in ookinetes compared to blood and gametocyte stages (Figure S3C). We used quantitative RT-PCR (qRT-PCR) to investigate whether the defect in microneme formation in the Δshlp1 ookinete is accompanied by downregulation of expression of genes encoding ookinete micronemal proteins in activated gametocytes and ookinetes. Of the three genes for micronemal proteins assayed, both *ctrp* and *soap* were significantly downregulated in Δshlp1 ookinetes ($p < 0.05$ and $p < 0.01$, respectively). Expression levels of the invasion-associated chitinase 1 (*cht1*) were completely unaffected in both stages (Figure 4D). Of the female-specific genes investigated, only *nek4* expression was significantly altered in Δshlp1 mutant ookinetes (Figure S3D).

A variety of micronemal proteins have previously been proposed to have a role in ookinete motility and ookinete to oocyst transition. CTRP deletion mutants are nonmotile and thus do not

form oocysts (Dessens et al., 1999; Yuda et al., 1999), while membrane attack ookinete protein (MAOP) (Kadota et al., 2004) and SOAP (Dessens et al., 2003) -null mutants are motile but unable or severely impaired in their capability to invade the midgut epithelium, respectively. To date, there is no information on the ultrastructure of these mutant parasites.

It is possible that the absence of micronemes is not due to a lack of cargo but incomplete maturation of the organelles or misdirected trafficking of the proteins as indicated by the diffuse overall staining of CTRP in the Δ*shlp1* cells. De novo biosynthesis of micronemes begins at the Golgi (Schrevel et al., 2008), which suggests a role for SHLP1 in the regulation of vesicular trafficking and microneme biogenesis. This suggestion is further corroborated by our colocalization and subcellular fractionation data showing SHLP1-GFP in the ER as a peripheral and integral membrane protein. Furthermore, while there is a marked effect on microneme development and ookinete function in the Δ*shlp1* mutant, there is no obvious developmental effect on the other invasive stages (i.e., sporozoites and merozoites) or on asexual development. However, the micronemes of the ookinete are structurally unique with a thin duct connecting the micronemes to the cell apex, a structure that is lacking in other developmental stages. Future studies are needed to understand the function of micronemal proteins and their secretion in the absence of micronemes.

The ability of ookinetes with no micronemes to invade the midgut epithelium has recently been described for a mutant lacking the paternally inherited MISFIT gene, corroborating our finding that mutants with a defect in microneme organelle biogenesis are capable of midgut invasion. However, our genetic complementation result showed that *shlp1* is inherited through the female line, in contrast to MISFIT that showed a paternal effect (Bushell et al., 2009).

In summary, our results indicate that SHLP1 in *Plasmodium* is essential for parasite transmission via the mosquito and thus a potential target for the development of transmission-blocking drugs. Ookinete-to-oocyst transition represents one of the biggest bottlenecks in the life cycle of the malarial parasite, and we show here that SHLP1 plays a crucial role in this process.

EXPERIMENTAL PROCEDURES

See Extended Experimental Procedures for details.

Ethics Statement

All animal work has passed an ethical review process and was approved by the United Kingdom Home Office. Work was carried out in accordance with the United Kingdom "Animals (Scientific Procedures) Act 1986" and in compliance with 'European Directive 86/609/EEC' for the protection of animals used for experimental purposes. The permit number for the project license is 40/3344.

Generation and Genotyping of Transgenic Parasites

To tag the endogenous *shlp1* at the C terminus with GFP, a single homologous recombination technique was used (Guttery et al., 2012a). To replace *shlp1* by double homologous recombination, a targeting vector was generated using the pBS-DHFR cassette (Tewari et al., 2010). See Extended Experimental Procedures for all oligonucleotide sequences and detailed methods.

Bioinformatic Analysis

Sequence alignments were performed using ClustalW2 and CLC Genomics Workbench (CLC bio, Cambridge, MA). The phylogenetic tree was generated using Fig Tree v1.3.1.

Phenotypic Analysis

Phenotypic screening was performed as previously described (Guttery et al., 2012a; Tewari et al., 2010). Briefly, asexual proliferation and gametocytogenesis were analyzed using blood smears. Gametocyte activation, zygote formation, and ookinete conversion rates were monitored in in vitro cultures using as a marker the surface antigen P28. For mosquito transmission, triplicate sets of 20–60 *Anopheles stephensi* were used.

Purification of Schizonts, Gametocytes, and Ookinetes

Schizonts, gametocytes, and ookinetes were purified as described previously (Guttery et al., 2012a).

Quantitative RT-PCR

Gene expression was quantified from 250 ng of total RNA as previously described (Guttery et al., 2012a). *hsp70* and *arginyl-tRNA synthetase* were used as reference genes. Primer sequences and cycling conditions are given in Extended Experimental Procedures.

Isolation of SHLP1-GFP Protein, Phosphatase Assay, and Subcellular Fractionation

Blood aliquots from parasite-infected mice were incubated in ookinete medium for 30 min at 20°C and processed for protein purification and phosphatase assay as described previously (Guttery et al., 2012a). Subcellular fractionation was performed using a carbonate method adapted from Hopp et al. (2012). Soluble (hypotonic lysis), peripheral membrane (carbonate soluble), and integral membrane (carbonate insoluble) fractions were analyzed by western blotting.

SHLP1 In Vivo Phosphorylation

Purified activated gametocytes and purified schizonts were metabolically labeled with 3–5 MBq ^{32}P-orthophosphate for 30 min at 20°C and processed for phosphorylation assay as described previously (Guttery et al., 2012a).

Injections of Ookinetes into the Mosquito Hemocoel and Genetic Crosses

Hemocoel injection of ookinetes and genetic complementation crosses were carried out as described previously (Ecker et al., 2008). See Extended Experimental Procedures for detailed methods.

Electron Microscopy, IFA, and ER Staining

Ookinetes cultured and purified as described above were fixed and processed for routine electron microscopy and IFAs were performed on air-dried ookinete slides from ookinete cultures as described recently (Guttery et al., 2012b). To stain for the ER, ER-Tracker Red (Invitrogen) was used at 2 μM. Blood stages were stained in schizont medium for 60 min at 37°C. Following complete conversion, ookinetes were stained in ookinete medium for 90 min at 25°C. Cells were washed once with respective medium and resuspended in PBS containing Hoechst 33342 DNA stain before being mounting for fluorescent microscopy.

Statistical Analyses

All statistical analyses were performed using GraphPad Prism (GraphPad Software). For phenotypic analysis, nonparametric Mann-Whitney U tests were used. For RNA expression levels, an unpaired t test was used. For genetic complementation experiments, Kruskal-Wallis one-way ANOVA with Dunn's multiple comparison post hoc test was used.

SUPPLEMENTAL INFORMATION

Supplemental Information includes Extended Experimental Procedures, three figures, one table, and two movies and can be found with this article online at http://dx.doi.org/10.1016/j.celrep.2013.01.032.

REFERENCES

Andreeva, A.V., and Kutuzov, M.A. (2004). Widespread presence of "bacterial-like" PPP phosphatases in eukaryotes. BMC Evol. Biol. 4, 47.

Bannister, L.H., and Sherman, I.W. (2009). Plasmodium. In Encyclopedia of Life Sciences (ELS) (Chichester, UK: Wiley).

Bushell, E.S., Ecker, A., Schlegelmilch, T., Goulding, D., Dougan, G., Sinden, R.E., Christophides, G.K., Kafatos, F.C., and Vlachou, D. (2009). Paternal effect of the nuclear formin-like protein MISFIT on Plasmodium development in the mosquito vector. PLoS Pathog. 5, e1000539.

Collins, F.H., Sakai, R.K., Vernick, K.D., Paskewitz, S., Seeley, D.C., Miller, L.H., Collins, W.E., Campbell, C.C., and Gwadz, R.W. (1986). Genetic selection of a Plasmodium-refractory strain of the malaria vector Anopheles gambiae. Science 234, 607–610.

Dessens, J.T., Beetsma, A.L., Dimopoulos, G., Wengelnik, K., Crisanti, A., Kafatos, F.C., and Sinden, R.E. (1999). CTRP is essential for mosquito infection by malaria ookinetes. EMBO J. 18, 6221–6227.

Dessens, J.T., Sidén-Kiamos, I., Mendoza, J., Mahairaki, V., Khater, E., Vlachou, D., Xu, X.J., Kafatos, F.C., Louis, C., Dimopoulos, G., and Sinden, R.E. (2003). SOAP, a novel malaria ookinete protein involved in mosquito midgut invasion and oocyst development. Mol. Microbiol. 49, 319–329.

Ecker, A., Bushell, E.S., Tewari, R., and Sinden, R.E. (2008). Reverse genetics screen identifies six proteins important for malaria development in the mosquito. Mol. Microbiol. 70, 209–220.

Guttery, D.S., Ferguson, D.J., Poulin, B., Xu, Z., Straschil, U., Klop, O., Solyakov, L., Sandrini, S.M., Brady, D., Nieduszynski, C.A., et al. (2012a). A putative homologue of CDC20/CDH1 in the malaria parasite is essential for male gamete development. PLoS Pathog. 8, e1002554.

Guttery, D.S., Poulin, B., Ferguson, D.J., Szöör, B., Wickstead, B., Carroll, P.L., Ramakrishnan, C., Brady, D., Patzewitz, E.M., Straschil, U., et al. (2012b). A unique protein phosphatase with kelch-like domains (PPKL) in Plasmodium modulates ookinete differentiation, motility and invasion. PLoS Pathog. 8, e1002948.

Hopp, C.S., Flueck, C., Solyakov, L., Tobin, A., and Baker, D.A. (2012). Spatio-temporal and functional characterisation of the Plasmodium falciparum cGMP-dependent protein kinase. PLoS ONE 7, e48206.

Hu, G., Cabrera, A., Kono, M., Mok, S., Chaal, B.K., Haase, S., Engelberg, K., Cheemadan, S., Spielmann, T., Preiser, P.R., et al. (2010). Transcriptional profiling of growth perturbations of the human malaria parasite Plasmodium falciparum. Nat. Biotechnol. 28, 91–98.

Kadota, K., Ishino, T., Matsuyama, T., Chinzei, Y., and Yuda, M. (2004). Essential role of membrane-attack protein in malarial transmission to mosquito host. Proc. Natl. Acad. Sci. USA 101, 16310–16315.

Kutuzov, M.A., and Andreeva, A.V. (2012). Prediction of biological functions of Shewanella-like protein phosphatases (Shelphs) across different domains of life. Funct. Integr. Genomics 12, 11–23.

Lasonder, E., Treeck, M., Alam, M., and Tobin, A.B. (2012). Insights into the Plasmodium falciparum schizont phospho-proteome. Microbes Infect. 14, 811–819.

McConnell, J.L., and Wadzinski, B.E. (2009). Targeting protein serine/threonine phosphatases for drug development. Mol. Pharmacol. 75, 1249–1261.

Mochida, S., and Hunt, T. (2012). Protein phosphatases and their regulation in the control of mitosis. EMBO Rep. 13, 197–203.

Moon, R.W., Taylor, C.J., Bex, C., Schepers, R., Goulding, D., Janse, C.J., Waters, A.P., Baker, D.A., and Billker, O. (2009). A cyclic GMP signalling module that regulates gliding motility in a malaria parasite. PLoS Pathog. 5, e1000599.

Moorhead, G.B., Trinkle-Mulcahy, L., and Ulke-Lemée, A. (2007). Emerging roles of nuclear protein phosphatases. Nat. Rev. Mol. Cell Biol. 8, 234–244.

Murray, C.J.L., Rosenfeld, L.C., Lim, S.S., Andrews, K.G., Foreman, K.J., Haring, D., Fullman, N., Naghavi, M., Lozano, R., and Lopez, A.D. (2012). Global malaria mortality between 1980 and 2010: a systematic analysis. Lancet 379, 413–431.

Opitz, C., and Soldati, D. (2002). 'The glideosome': a dynamic complex powering gliding motion and host cell invasion by Toxoplasma gondii. Mol. Microbiol. 45, 597–604.

Schrevel, J., Asfaux-Foucher, G., Hopkins, J.M., Robert, V., Bourgouin, C., Prensier, G., and Bannister, L.H. (2008). Vesicle trafficking during sporozoite development in Plasmodium berghei: ultrastructural evidence for a novel trafficking mechanism. Parasitology 135, 1–12.

Sebastian, S., Brochet, M., Collins, M.O., Schwach, F., Jones, M.L., Goulding, D., Rayner, J.C., Choudhary, J.S., and Billker, O. (2012). A Plasmodium calcium-dependent protein kinase controls zygote development and transmission by translationally activating repressed mRNAs. Cell Host Microbe 12, 9–19.

Siden-Kiamos, I., Ecker, A., Nybäck, S., Louis, C., Sinden, R.E., and Billker, O. (2006). Plasmodium berghei calcium-dependent protein kinase 3 is required for ookinete gliding motility and mosquito midgut invasion. Mol. Microbiol. 60, 1355–1363.

Solyakov, L., Halbert, J., Alam, M.M., Semblat, J.P., Dorin-Semblat, D., Reininger, L., Bottrill, A.R., Mistry, S., Abdi, A., Fennell, C., et al. (2011). Global kinomic and phospho-proteomic analyses of the human malaria parasite Plasmodium falciparum. Nat Commun 2, 565.

Tewari, R., Straschil, U., Bateman, A., Böhme, U., Cherevach, I., Gong, P., Pain, A., and Billker, O. (2010). The systematic functional analysis of Plasmodium protein kinases identifies essential regulators of mosquito transmission. Cell Host Microbe 8, 377–387.

Tsuruta, H., Mikami, B., Yamamoto, C., and Yamagata, H. (2008). The role of group bulkiness in the catalytic activity of psychrophile cold-active protein tyrosine phosphatase. FEBS J. 275, 4317–4328.

Uhrig, R.G., and Moorhead, G.B. (2011). Two ancient bacterial-like PPP family phosphatases from Arabidopsis are highly conserved plant proteins that possess unique properties. Plant Physiol. 157, 1778–1792.

Ward, P., Equinet, L., Packer, J., and Doerig, C. (2004). Protein kinases of the human malaria parasite Plasmodium falciparum: the kinome of a divergent eukaryote. BMC Genomics 5, 79.

Wilkes, J.M., and Doerig, C. (2008). The protein-phosphatome of the human malaria parasite Plasmodium falciparum. BMC Genomics 9, 412.

Yuda, M., Sakaida, H., and Chinzei, Y. (1999). Targeted disruption of the plasmodium berghei CTRP gene reveals its essential role in malaria infection of the vector mosquito. J. Exp. Med. 190, 1711–1716.